Lab on a Chip

CRITICAL REVIEW

View Article Online
View Journal | View Issue

Cite this: *Lab Chip*, 2015, **15**, 4500

Microfluidic devices to enrich and isolate circulating tumor cells

J. H. Myung[a] and S. Hong*[ab]

Received 8th August 2015,
Accepted 28th October 2015

DOI: 10.1039/c5lc00947b

www.rsc.org/loc

Given the potential clinical impact of circulating tumor cells (CTCs) in blood as a clinical biomarker for the diagnosis and prognosis of various cancers, a myriad of detection methods for CTCs have been recently introduced. Among those, a series of microfluidic devices are particularly promising as they uniquely offer micro-scale analytical systems that are highlighted by low consumption of samples and reagents, high flexibility to accommodate other cutting-edge technologies, precise and well-defined flow behaviors, and automation capability, presenting significant advantages over conventional larger scale systems. In this review, we highlight the advantages of microfluidic devices and their potential for translation into CTC detection methods, categorized by miniaturization of bench-top analytical instruments, integration capability with nanotechnologies, and *in situ* or sequential analysis of captured CTCs. This review provides a comprehensive overview of recent advances in CTC detection achieved through application of microfluidic devices and the challenges that these promising technologies must overcome to be clinically impactful.

1. Introduction

Circulating tumor cells (CTCs) in cancer patients' blood have shown promise as a clinical biomarker for cancer diagnosis, prognosis, prediction, stratification and pharmacodynamics without invasive tissue biopsy.[1–3] According to 'seed and soil' theory,[4] CTCs that escaped from primary tumor sites travel through the bloodstream until they either extravasate and initiate secondary tumor colonies or die. Over the past decade, a number of technologies have been developed to discriminate CTCs that are distinct from normal hematological cells based on their biological and/or physiochemical properties.[5,6] Among these technologies, CellSearch® and Gilupi, approved by the US FDA and the EU, respectively, are in advanced stages of clinical translation. CellSearch® (Janssen Diagnostics), a semi-automated CTC detection system approved for breast, prostate, and colorectal metastatic cancers, relies on the immunomagnetic separation of CTCs using an antibody against a CTC marker, epithelial cell adhesion molecule (EpCAM).[1] Gilupi is an *in vivo* CTC isolation system for CTC quantification and *ex vivo* post-capture analysis *via* insertion of a CellCollector tip functionalized with polymers and anti-EpCAM into the blood vessel.[7] However, the rarity (approximately one CTC in the background of 10^6–10^9 hematologic cells), epithelial–mesenchymal plasticity and heterogeneity of CTCs have hampered clinically reliable detection and molecular characterization of CTCs.[8,9]

A variety of emerging microfluidic devices have introduced several important advantages and enhancement to existing CTC capture strategies, including size-based and dielectrophoresis-based separation, immunoaffinity-based capture, fluorescence-based sorting and immunomagnetic capture of CTCs, as comprehensively reviewed earlier by others.[10–16] Many kinds of materials, such as polymers (*e.g.* polydimethylsiloxane (PDMS)), ceramics (*e.g.* glass), semi-conductors (*e.g.* silicon) and metals, have been used to develop microfluidic devices for CTC capture. Among these, due to its optical characteristics, biological and chemical compatibility, fast prototyping and cost efficiency,[17] PDMS allows easy fabrication of microfluidic devices using standard photolithography and their integration with other nanotechnologies. As a result, PDMS has been the most commonly used material for microfluidic devices employed for the detection and isolation of CTCs particularly in their early developmental stages.[18] Although highly promising, in order for microfluidic devices to be successfully translated, several limitations, such as batch-to-batch variations, slow processing speed of rare cells in large sample volumes and non-specific binding, must be overcome.[19]

In this review, we focus on how the advantages of microfluidic devices have been exploited to enhance CTC enrichment and detection. The advantages of microfluidic devices and their recent examples are summarized in Table 1. The recent microfluidic device techniques implemented to CTC devices are classified into three principal approaches based

[a] *Department of Biopharmaceutical Sciences, College of Pharmacy, University of Illinois, 833 S. Wood St., Chicago, IL, 60612, USA. E-mail: sphong@uic.edu*
[b] *Division of Integrated Science and Engineering and Department of Integrated OMICs for Biomedical Sciences, Yonsei University, Seoul, 03706, Korea*

Table 1 The advantages of microfluidic devices for enhancing CTC enrichment and detection, and their related recent examples

Advantages	Related properties	Applications	Examples
Miniaturization of conventional, bench-top instruments for cell sorting	• Small amounts of samples and reagents required	• Microfilters for size-based separation	Ref. 22–31
	• Well-controlled fluidic behaviour	• Micro-centrifuge for density-based separation	Ref. 33, 34
	• Easy to design, modify and fabricate the devices	• Micro-immunoassay	Ref. 37, 38
	• Transparent, soft and flexible	• Micro-MACS	Ref. 39–45
		• Micro-FACS	Ref. 46, 47
Integration capability with other nanotechnologies	• Surface functionalization using silanes	• Integration with nanostructured surface	Ref. 55–57
	• Transparent, soft and flexible	• Combination with magnetic beads	Ref. 58, 59
		• Integration with polymers to enhance CTC capture and release efficiencies	Ref. 66–70
In situ post-capture analysis	• High gas permeability (especially to CO_2 rather than O_2)	• *In situ* analysis	Ref. 75, 76
	• Transparent, soft and flexible	• Sequential analysis after release of the cells	Ref. 74, 78

on the roles that microfluidic technology plays in CTC enrichment and detection: (i) miniaturization of conventional, bench-top instruments for cell sorting; (ii) integration with nanotechnologies for improved performance; (iii) enabling *in situ* post-capture analysis. Within each category, several subsections are also provided to further categorize each technology based on its detection/functional mechanisms. In addition, we discuss key challenges that microfluidic CTC devices encounter, which should be overcome in order for this promising technology to be clinically impactful.

2. Roles of microfluidics in CTC enrichment and detection

Microfluidic technology can be considered as both a study of fluidic behaviors in microchannels and a manufacturing method for microfluidic devices. A microfluidic device typically manipulates small amounts (10^{-6} to 10^{-12} L) of fluid using 1 to 1000 μm channel sizes. Microfluidic systems with small sample volumes, multiplexing capabilities and large surface-area-to-volume ratios offer a unique way to capture and detect rare CTCs. Specifically, microfluidic devices enable (i) the use of very small quantities of samples and reagents to carry out highly sensitive detection, (ii) facile integration with other technologies that improve the efficiency of the device and (iii) a one-step process of sample loading, separation and analysis.

2.1. Miniaturization

Microfluidic devices are originally designed for miniaturization in chemistry, physics, biology, materials science and bioengineering from the mm-scale to the μm-scale. The majority of conventional CTC detection methods, such as magnetic-activated cell sorting (MACS), fluorescence-activated cell sorting (FACS), high-definition fluorescence scanning microscopy, isolation by size of epithelial tumor cells (ISET) and density-gradient cell sorting using a centrifuge, are designed as bench-top instruments. Microfluidic systems have been recently developed to provide miniaturized structures and integrated processing capabilities by down-scaling such bench-top instruments.[20,21] Compared to bench-top instruments, CTC microfluidic devices require only a small amount of reagents, enable superior sensitivity to be achieved, and enhance enrichment on small surface areas. As a result, CTC microfluidic devices enable cost-effective, simple and automated operation, along with precise control over the flow behaviors and biological interactions of CTCs in microchannels.[14,20]

2.1.1. Microfilters for size-based separation. Based on the morphological and size differences between cancer cells (15–40 μm in diameter) and leukocytes (≤10 μm in diameter), size-based filtration using either polymer membranes or microsieve membrane filter devices made of silicon or nickel has been shown to extract CTCs from whole blood samples.[22–26] The size, geometry and density of the pores in the microfilters can be uniformly and precisely controlled.[23] Along with batch fabrication, this technology can also afford maximal sample processing capability through parallel arrays of multiple flow cells, which reduces processing time, cost and filter clogging, while facilitating mass production and high-throughput screening for large-scale clinical studies.[26] A silicon microsieve device with a high-density pore array was able to rapidly filter tumor cells from whole blood.[24] The highly porous structure (~5000 pores of 10 μm diameter per mm^2) of the thin silicon membrane (30 μm in thickness, 10^5 pores per device) minimized the fluid resistance, allowing rapid CTC filtration at a high flow rate of 1 mL min^{-1} (Fig. 1a–c). From the cancer cell-spiked human whole blood sample, more than 80% of MCF-7 and HepG2 cells were recovered at a rapid flow rate of 1 mL min^{-1}. The device was further validated with blood from cancer patients. The whole process, from loading of blood samples drawn from various cancer patients (8 samples) to CTC counting, was completed in 1.5 h. In addition, the rigid silicon structure and small device footprint (5 mm in diameter) allowed *in situ*

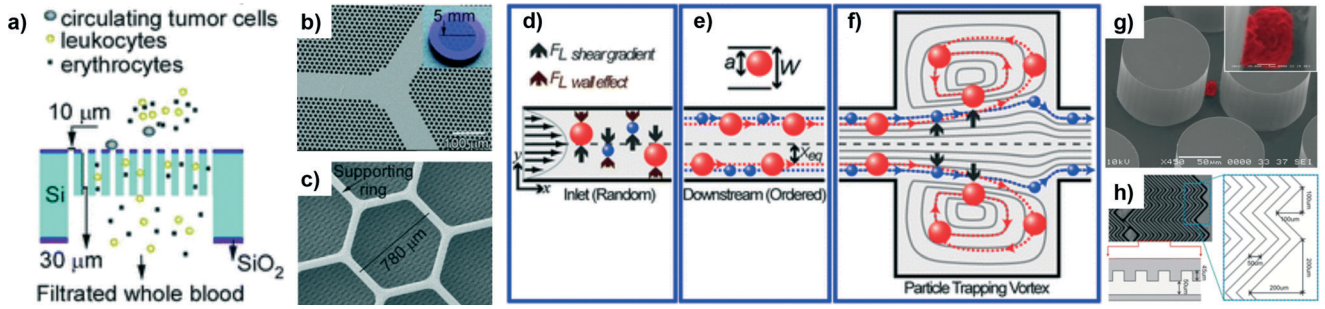

Fig. 1 Miniaturization of a filter, a centrifuge and an immunoassay for CTC detection. (a) A schematic illustration of size-based CTC separation using a silicon microsieve. The diameter of the fabricated microsieve is around 5 mm (b), which includes micropores of 10 μm diameter and a supporting ring as shown in the SEM image (c). The fabricated microfilter is sandwiched between the microscope plate and the blood reservoir, and whole blood was injected into the microsieve filter using a peristaltic pump (reproduced with permission from the Royal Society of Chemistry). (d–f) A scheme of the separation mechanism of cells with different densities in a microcentrifuge. After being injected into the microchannels, the cell mixtures were subjected to a shear gradient lift force, which directs particles toward the channel wall, and a wall effect lift force, directed toward the channel center (d). The balance between the shear gradient and wall effect lift forces near dynamic equilibrium positions (e), X_{eq}, was broken when the lift forces were decoupled near the particle trapping chamber (f), and the CTCs were separated from the blood cells (reproduced with permission from the Royal Society of Chemistry). (g and h) The miniaturized immunoassay, CTC-chip with a micropost array (1st generation, g) and herringbone patterns (2nd generation, h) were able to capture CTCs from whole blood after being functionalized with anti-EpCAM on the silicon (g) or PDMS (h) surface, for point-of-care isolation of CTCs from peripheral blood (reproduced with permission from Nature Publishing Group (g) and the National Academy of Sciences (h)).

immunostaining for CTC identification directly on the microsieves. However, considering that the size of most CTCs in clinical samples widely varies and is often found to be similar to that of leukocytes, as opposed to that of *in vitro* cancer cell lines,[27,28] these size-based microfiltration systems for CTC detection require further validation with clinical samples.

It is noteworthy that it has been reported that CTCs which form clusters are more invasive and metastatic than CTCs that are present in their single-cell form.[29,30] As a result, methods to isolate CTC clusters from blood have been developed.[30,31] For example, Cluster-Chip utilizes a microfluidic device integrated with specialized bifurcating traps.[31] The PDMS-based microfluidic device consisted of 4096 parallel tracks, and each CTC-cluster trap was composed of multiple rows of shifted triangular pillars.[31] The preliminary data obtained using MDA-MB-231 cell cluster-spiked human blood revealed that the Cluster-Chip showed higher capture efficiency (near 100%) at 2.5 mL h^{-1}, in direct comparison with 5 μm membrane filters (only ~26% at 0.1 psi). Because the Cluster-Chip is immunolabeling-independent and is composed of shifted triangular pillars, 80% of the captured CTC clusters were released from the Cluster-Chip by simply reversing the flow and transiently cooling the samples to 4 °C. The captured CTC clusters from blood samples of breast cancer, melanoma or prostate cancer patients were also used for subsequent RNA sequencing and immunostaining, which showed low expression levels of transcripts encoding CTC markers, such as keratins, MUC1, EpCAM, and CDH1.[31]

2.1.2. Micro-centrifuge. Based on the distinct size and density differences between cancer cells and leukocytes, the miniaturized micro-centrifuge, or centrifuge-on-a-chip, can also isolate CTCs from whole blood samples.[32] Typical bench-top centrifuges are widely used for separation of cells by size/density, particularly during sample preparation. The micro-centrifuge with a μL-scale channel volume can replicate the functions of a conventional centrifuge simply relying on a purely fluid dynamic phenomenon.[32] The well-controlled flow behaviors in microchannels selectively separate and trap CTCs in microscale vortices without moving parts or external forces. Because of its high parallel processing capability, this technology can also shorten processing time, reduce cost and filter clogging, and enable high-throughput screening for clinical studies.[32,33]

A micro-centrifuge with laminar fluid microvortices has been demonstrated to continuously trap and enrich cancer cells from spiked blood samples using hydrodynamic forces.[33] At a speed of 5 mL min^{-1}, the balance and decoupling of a shear gradient lift force and a wall effect lift force in laminar vortices and microvortex chambers induced particle entry and trapping within the microvortex chambers, as depicted in Fig. 1d–f. Without the need for manual pipetting and washing steps, the micro-centrifuge was reported to enrich rare cancer cells from blood samples with minimal cytotoxicity (~90% cell viability). The capability of on-chip fluorescence labeling of intra- and extra-cellular antigens also enabled the identification and quantification of the trapped cancer cells (~40% capture purity). This simple micro-centrifuge could be potentially used to develop an automated, low-cost and high-throughput system for CTC enrichment as an alternative to the standard bench-top centrifuge used for standardized clinical diagnostics in resource-poor settings.[34]

2.1.3. Miniaturized immunoassay. Conventional immunoarray systems, such as the enzyme-linked immunosorbent assay (ELISA), can be integrated with portable microfluidic devices. Immunoassay is one of the main analytical techniques used in biomedical applications due to the highly sensitive and selective binding properties of antigen–antibody interaction, which allow for specific analyte detection.[35] However,

conventional immunoassays require a labor-intensive process involving multiple reagent treatment/incubation and several washing steps. To address this issue, the conventional immunoassay has been miniaturized on microfluidic devices to control binding kinetics, reduce reagent consumption and automate the process with precise control.[35,36] The surface of a PDMS microfluidic device can be functionalized with silanes to immobilize proteins, polymers and inorganic materials (more details in section 2.2).[5,6] Compared to antibody-free detection methods using microfilters and microcentrifuges described in the previous sections, an immunoarray, similar to micro-MACS and micro-FACS described in later sections, requires specific antibodies against surface markers on target cells. EpCAM has been the most commonly used capture agent in these devices because of its overexpression in various CTCs with epithelial origin, but no expression in normal hematologic cells.

The CTC capture efficiency of microfluidic immunoassay devices can be further enhanced by modifying hydrodynamic mixing efficiency in the microfluidic devices. Toner/Haber's group has developed a microfluidic device called the CTC-chip, which is in its advanced stage of development (Fig. 1g and h).[37,38] The CTC-chip showed great potential for simple and cost-effective CTC detection. The silicon (1st generation) and PDMS (2nd generation) chip surfaces were modified using a series of chemicals, *i.e.*, (3-mercaptopropyl)-trimethoxysilane (MPTMS), *N*-γ-maleimidobutyryl-oxysuccinimide ester (GMBS), NeutrAvidin and biotinylated anti-EpCAM. Microposts incorporated into the fluidic channels (1st generation) enhanced the hydrodynamic efficiency of the flow, resulting in sensitive detection of CTCs under flow.[37] Although the micropost-based system exhibited a high capture yield at a low flow rate (1–2 mL h^{-1}), the capture yield substantially decreased with an increase in flow rate (higher than 2.5 mL h^{-1}) due to the insufficient time for CTCs to bind to the surface. It has been also reported that the first generation of the CTC-chip showed poor mixing efficiency of viscous flow due to low diffusivity. In an effort to address these issues, subsequent studies have incorporated herringbone patterns onto the ceiling of the 2nd generation microfluidic device, increasing the mixing efficiency.[38] Modifications on the microchannel surfaces, such as microposts and 2-dimensional grooves, have been shown to be effective in increasing the contact surface area and disrupting the laminar flow to maximize collisions between the CTCs and antibody-coated surfaces, enhancing the overall CTC capture efficiency.[38] However, these modifications could cause non-specific capture or clogging of CTC clusters[38] at the regions where the flow is locally rotating or the local shear stress is low.

2.1.4. Micro-MACS. Micro-MACS is one of the most widely used approaches for CTC detection. Compared to conventional bench-top MACS, a downscaled microfluidic system provides a well-confined flow and magnetic field because its short vertical height and large cross-section help to increase the sensitivity of magnetic capture.[21] Similar to the conventional MACS system for CellSearch®, a microfluidic-based immunomagnetic assay uses antibody-conjugated magnetic beads and an external magnetic field for capture. However, one unique difference of micro-MACS is that, depending on the direction of the magnetic field, the collection location of the target cells can be controlled (inside or outside the microfluidic devices). For example, a device reported by the Ingber lab retained the captured CTCs on the chip for *in situ* post-capture analysis.[39] It has also been reported that magnetically driven collection of CTCs can be controlled to be located at different outlets.[40] Although the potential cytotoxicity of the surface-bound magnetic beads should be addressed, micro-MACS has great potential for high-throughput screening and commercial translation. Captured viable CTCs using magnetic nanoparticles (MNPs) in micro-MACS can be easily released and recovered by removing a magnet. However, magnetic-activated sorting of cells from whole blood may change the cell function or activity after binding with the paramagnetic beads.[41]

The use of MNPs to magnetically capture and identify CTCs has been shown to efficiently lead to CTC isolation using micro-MACS. After conjugation with anti-EpCAM, Fe_3O_4 MNPs were added to cancer cell-spiked blood samples in a manner identical to the procedure of the bench-top CellSearch™ system.[42] As an external force, a defined magnetic field gradient in the vicinity of arrayed magnets with alternating polarities, as illustrated in Fig. 2a, was applied to a typical PDMS microfluidic chip. This micro-MACS led to the effective capture of MNP-labeled cancer cells, resulting in 90% and 86% recovery rates of an $EpCAM^{low}$ colon cancer cell line, COLO205, and an $EpCAM^{high}$ breast cancer cell line, SKBR3 cells, respectively.[42] Compared to the CellSearch™ system, this micro-MACS required 25% fewer magnetic particles to achieve a comparable capture rate, while maintaining a fast screening speed (at an optimal blood flow rate of 10 mL h^{-1}).[42]

Under a magnetic field, a microfluidic device with a main channel and multiple collection-channels lined in dead-end side chambers was demonstrated to isolate and trap magnetic bead-bound CTCs.[39] First, CTCs in blood were labeled with anti-EpCAM-coated magnetic microbeads (2.8 μm in diameter). Then, the magnetically labeled CTCs were isolated within the dead-end side chambers of the micro-MACS device with an angled inlet conduit (Fig. 2b). The design and dimensions of the microfluidic channels were optimized to maximize the capture efficiency and protect the isolated cells from shear stress and stress-induced changes in cell physiology and behavior such as proliferation. This micro-MACS device was able to isolate CTCs from mouse blood with high efficiency (~90%), specificity (0.4% blood cell capture) and viability (~90%). Additionally, the captured CTCs within its dead-end side chambers were expanded in culture after the removal of magnets from the device.

Magnetically driven collection of CTCs can be combined with cell sorting using a hydrodynamic flow created in a microfluidic device. For instance, after immunolabeling of

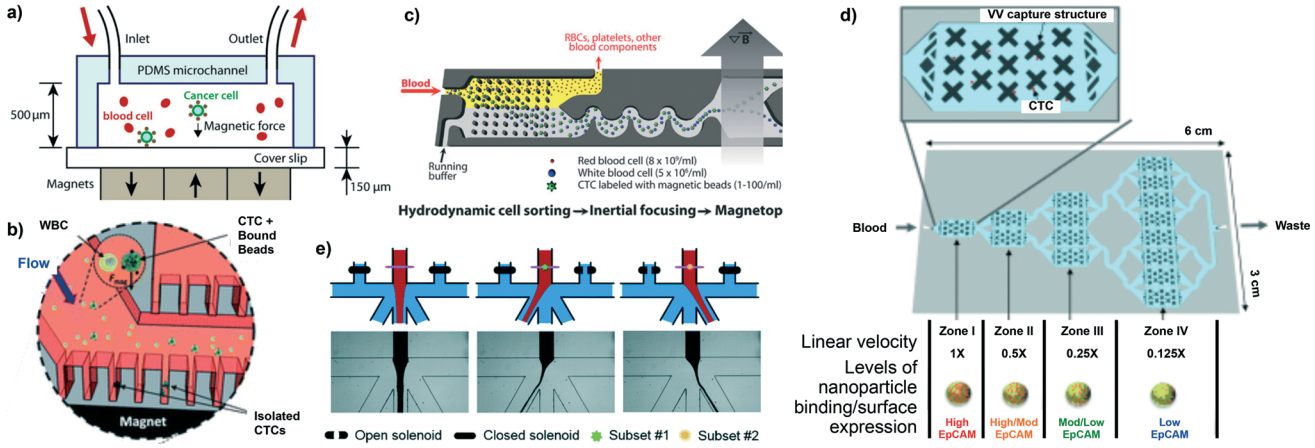

Fig. 2 Recent applications of micro-MACS and micro-FACS for CTC capture and identification. (a) A schematic illustration of CTC separation in the microchannel under a magnetic field after labelling with anti-EpCAM-functionalized magnetic nanoparticles (reproduced with permission from the Royal Society of Chemistry). (b) The magnetic nanoparticle-bound CTCs were isolated in a unique microfluidic device containing an angled inlet channel and collection channels. The collection channels in the microchannel have arrays of dead-end side chambers (50 × 6 × 50 μm square with a gap of 100 μm) due to a permanent magnet beneath the lower row of the side chambers (reproduced with permission from the Royal Society of Chemistry). (c) The magnetic nanoparticle-bound CTCs were sorted out from blood cells in a series of debulking, inertial focusing and magnetic separation steps in the CTC-iChip system (reproduced with permission from the American Association for the Advancement of Science). (d) Depending on the EpCAM-expression level on CTCs, the anti-EpCAM-magnetic nanoparticle-labeled CTCs were sorted in a device with multiple velocity valley zones with different linear velocities: $EpCAM^{High}$ cells trapped in zone I and $EpCAM^{Low}$ cells trapped in zone IV (reproduced with permission from Wiley-VCH Verlag GmbH & Co. KGaA, Weinheim). (e) The separation mechanism of micro-FACS, dual-capture eDAR. After immunostaining blood samples, the active sorter in the microfluidic device was able to simultaneously separate the samples into 3 different channels: non-labeled to the center waste channel (left), green-labeled cells to the left isolation channel (middle) and red-labeled cells to the right isolation channel (right) (reproduced with permission from the Royal Society of Chemistry).

either CTCs or leukocytes using MNPs, inertial focusing in a microchannel induced alignment of CTCs and leukocytes, following debulking that removed erythrocytes, platelets and free MNPs (Fig. 2c). This alignment process allowed continuous, high-throughput separation of the nucleated cells.[40,43] The CTCs were then separated from leukocytes by either positive or negative selection using magnetophoresis.[40,43] Another example shown in Fig. 2d utilized local velocity valleys (VVs) generated in a multizone microfluidic device to sort a cancer cell mixture into several subpopulations depending on the levels of EpCAM expression.[45] The multizone microfluidic device consisted of four different regions with different linear velocities: $EpCAM^{high}$ cells trapped in zone I (1× speed), $EpCAM^{medium}$ cells trapped in zones II and III (0.5× and 0.25× speed), and $EpCAM^{low}$ cells trapped in zone IV (0.125× speed). The surface-marker-guided sorting and profiling of target cells in the multizone microfluidic device were successfully applied to *in vitro* cancer cell lines with varying levels of surface expression as well as clinical blood samples from prostate cancer patients.[45]

2.1.5. Micro-FACS. FACS has been widely used to sort heterogeneous mixtures of cells into multiple populations of a pure cell suspension based on fluorescence signals. FACS is automated, robust and specific with outstanding sorting speeds (up to 50 000 cells per second). Similar to MACS which relies on magnetic labels and magnets, FACS requires sequential steps of fluorescence labeling, hydrodynamic flow focusing, laser detection and cell sorting.[31] However, because of the lack of detection sensitivity to separate rare cells, FACS is usually considered to be more suitable to sort out cells that represent a relatively major portion in the mixture.[12]

Recent development in nanotechnology and microfluidic technology enables the miniaturization of bench-top FACS systems. For example, to adapt FACS for CTC isolation, Chiu's group developed a process called "ensemble-decision aliquot ranking" (eDAR) and applied it to micro-FACS.[46,47] Similar to FACS, target cells were first labeled with fluorescence-tagged antibodies. However, different from the simultaneous cell analysis and sorting in conventional FACS, the eDAR process divided the sample into aliquots containing thousands of cells, and then detected fluorescent CTCs in each aliquot with pulsed lasers (Fig. 2e). The virtual aliquot volume in eDAR was optimized at 2 nL for the system throughput (3 mL h^{-1}), which resulted in a capture efficiency of around 93% for both MCF-7 and SKBR-3 cells at a low concentration of 5 cells per mL. In addition, by utilizing multiple light sources and detectors as well as a variable-direction high-speed active sorter, eDAR simultaneously and selectively performed multi-color sorting of two cell subsets. A heterogeneous mixture of rare cells from whole blood was labeled with two types of fluorescence-tagged antibodies against EpCAM and the epidermal growth factor receptor (EGFR). The dual capture eDAR device with an active sorter demonstrated the simultaneous isolation of EpCAM+ and EGFR+ cancer cells with improved recovery yields (~88%) at 50 μL min^{-1}.

Multiple functions can be successfully integrated into highly interdisciplinary microfluidic devices; however, this

multifunctionalization often makes the design, fabrication and operation of the devices complicated. The fabrication of complex devices would require technical expertise and long preparation time, and would be challenging to scale up for volume production and large-scale clinical applications.[19] Methods that require the use of hard-to-fabricate devices may have issues related to inconsistency in quality control, analytical validation and device fabrication for their clinical acceptance.[19,48] Furthermore, these structured microchannels would require a long time for full-field scanning to find the cells captured at vertically different locations.[49] In order to truly benefit from miniaturization for CTC detection, other instruments used in the detection process (*e.g.* a fluorescence detector with laser sources and optics) also need to be modified for wide-field imaging for low-frequency high-throughput CTC detection without scarifying the image resolution.[49]

The turnaround time of microfluidic devices also needs to be improved for high-throughput analysis of clinical samples. Due to the rarity of CTCs in blood, a fixed volume of 7.5 mL of blood is typically processed for CTC capture as CellSearch® does. The volume capacity of a microchannel is typically less than 100 μL, which is too small to process 7.5 mL of blood within a reasonable time.[20] Even without considering the time to stain and scan the chip to find and count CTCs among a large number of hematological cells, it could take several hours to process the blood from a single patient.[20] It is a challenge for clinical laboratories to complete clinical-scale samples for CTC detection as a routine assay at this sample processing speed.[19] Moreover, this long turnaround time, in addition to high shear stress and the potential clogging issue of blood clots or CTC clusters in microchannels, may adversely affect the viability and function of captured CTCs, making phenotyping and genotyping difficult.[20,50]

2.2. Integration capability of microfluidic devices

Another important aspect of PDMS microfluidic devices is that they can be easily integrated with nanotechnologies to improve their performance, owing to their several unique characteristics, such as (i) rapid fabrication by casting the PDMS polymer against photolithography-based molds,[51] (ii) optical transparency and high elasticity,[52] (iii) low magnetic susceptibility of PDMS polymers[52] and (iv) facile surface functionalization using silanes. The characteristic rapid and inexpensive prototyping of PDMS microfluidic devices with high fidelity can reduce time and cost for a design cycle, as well as enable the fabrication and testing of several prototypes to optimize design parameters such as the channel size and geometry. Elastomeric and optically transparent PDMS is an excellent material to be used under pressure since its surface can withstand high pressure under flow without deformation and can be easily observed under a microscope. Thus, PDMS microfluidic chambers with these characteristics can be integrated with nanostructured substrates functionalized for CTC capture. Low magnetic susceptibility could be useful in systems for transport, positioning, separation and sorting of magnetically labeled CTCs using magnetic forces, which can be combined with magnetic bead-based CTC detection. Hydrophilic silanol groups (Si–OH) can be easily derived on the hydrophobic surface of PDMS from its repeating unit of $–O–Si(CH_3)_2–$ *via* exposure to air and oxygen plasma oxidation.[51] The surface of PDMS or glass substrates could be functionalized with self-assembled monolayers of silanes, which can be further chemically modified.[51] In addition, the functionalized PDMS devices are prone to wetting with aqueous solutions and do not easily allow adsorption of other hydrophobic species. The capability of PDMS to undergo surface functionalization is suitable for the development of multifunctional microfluidic devices *via* addition of polymers for controlled surface chemistry and additional functions (*e.g.* releasing capability of captured cells). For these reasons, PDMS microfluidic devices can easily adapt integrated analytical systems for CTC separation.

2.2.1. Integration with nanostructured substrates. Nanostructured silicon substrates with highly dense arrays of uniform vertical silicon nanowires exhibit a high surface-to-volume ratio and enhanced sensitivity for biomolecule detection in biosensors.[53,54] Silicon nanowire arrays (SiNWAs) have unique structural features, excellent electronic, optical, thermoelectric and mechanical properties, and biocompatibility, as well as potential for various biomedical applications.[54] For example, compared with flat silicon substrates, SiNWAs with large surface areas were used as a platform for the enhanced capture of CTCs through incorporation into a PDMS microfluidic device.[55]

Anti-EpCAM-coated SiNWAs with a specific 3D nanostructure were integrated into a microfluidic system, called the NanoVelcro chip, to increase the cell–substrate contact frequency and improve the CTC-binding affinity.[56] After curing with aminosiloxane, the 3D surface of the SiNWAs and the integrated microfluidic devices were conjugated with streptavidin and biotinylated anti-EpCAM. This NanoVelcro system contained patterned SiNWAs coated with anti-EpCAM for high-affinity cell enrichment and a microfluidic device with a serpentine chaotic mixing channel capable of improving the CTC/substrate contact frequency (Fig. 3a). The synergistic effects led to high CTC-capture performance observed for both spiked and clinical blood samples, which could potentially provide a convenient and cost-efficient alternative for sorting CTCs in clinical laboratories. After modifications with thermally responsive polymers, CTC capture and release from the NanoVelcro system were well controlled upon external temperature changes.[57] This thermally responsive NanoVelcro system demonstrated the effective capture of tumor cells from blood at 37 °C and release of the captured cells with retained viability and functionality at 4 °C, which will be further described in section 2.2.4, which discusses the incorporation of releasing capability.

2.2.2. Combination with magnetic beads. Magnetic NPs can form self-assembled structures in microfluidic devices under a magnetic field and be functionalized for CTC

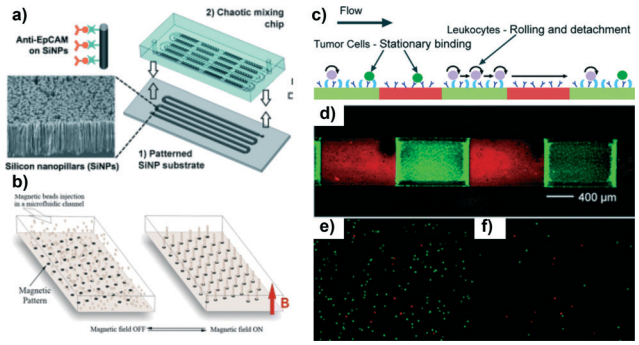

Fig. 3 Application examples of microfluidic devices integrated with nanotechnology for CTC capture. (a) A PDMS microfluidic device with a microchannel was assembled with nanostructured silicon arrays, which was further functionalized with anti-EpCAM for CTC capture. The increased surface area through integration with a nanostructured surface demonstrated enhanced CTC sensitivity, compared to a flat chip (reproduced with permission from Wiley-VCH Verlag GmbH & Co. KGaA, Weinheim). (b) Anti-EpCAM-coated magnetic nanoparticles were injected and arrayed inside a microfluidic device under an external vertical magnetic field, which was used to functionalize the microfluidic device for CTC capture as well as to release the captured CTCs after removing the magnet (reproduced with permission from the National Academy of Sciences). (c–f) A micropatterned microfluidic device integrated with nanomaterials and biomimetic proteins, such as dendrimers and E-selectin, respectively, significantly increases the CTC capture efficiency and purity under flow conditions. The alternating pattern of immobilized anti-EpCAM–dendrimer (red, d) and E-selectin (green, d) on a PDMS channel surface showed stationary tumor cell binding (red dots, e) across the entire capture surface, while leukocytes rolled (green dots, e) on the E-selectin patterns. After rinsing with a leukocyte elution buffer, the enrichment of red-labeled tumor cells on the surface was clearly shown in (f) (reproduced with permission from the American Chemical Society).

capture. Ephesia, a system of microfluidic channels with arrays of self-assembled biofunctionalized superparamagnetic beads, was developed using a hexagonal array of magnetic ink patterned at the bottom of a PDMS microfluidic channel after injecting anti-EpCAM-coated magnetic beads into the channel.[58] Upon exposure to the vertically applied external magnetic field, three-dimensional arrays of bead columns were formed and localized on top of the magnetic ink dots (Fig. 3b).[58] The integrated magnetic beads increased the amount of anti-EpCAM per surface area to efficiently bind to CTCs. The captured cells from blood samples taken from patients in the Ephesia system were released for post-capture analysis of mutation detection by removing a magnet.[59] For example, heterozygous E545K mutation in exon 9 of the PIK3CA gene was monitored on the released CTCs, which revealed the potential of this technology for post-capture genotyping.[59]

2.2.3. Addition of polymers for controlled surface chemistry. Recent advances in polymeric nanomaterials have enabled the design of biomedical devices with significantly improved performance. For example, multivalent binding that occurs in a variety of physiological processes has been exploited to significantly increase the sensitivity and selectivity of detection assays.[60] We have used poly(amidoamine) (PAMAM) dendrimers that allow precise control of the multivalent binding effect through their characteristic properties obtained from their well-defined chemical structure, high density of peripheral functional groups and easy deformability.[61,62] The binding strength between CTCs and a capture surface can be enhanced through the dendrimer-mediated multivalent binding effect, which can significantly improve the sensitivity and selectivity of the surfaces for CTC detection.[62,63] Compared to linear polymer-coated surfaces, the surfaces functionalized with the anti-EpCAM–dendrimer conjugates exhibited dramatically enhanced cell adhesion and binding stability towards three breast cancer cell lines (MDA-MB-361, MCF-7 and MDA-MB-231).[62] In addition, immobilization of E-selectin induced cell rolling and has been shown to enhance the surface capture of tumor cells (up to 10-fold compared to the same surface without dendrimers).[63–65] We have also applied the significant enhancement of the dendrimer-coated surfaces to various antibodies and have shown the effectiveness of the device in capturing tumor cells from clinically relevant blood samples as well.[63]

The biomimetic combination of the anti-EpCAM–dendrimer conjugates and E-selectin has been introduced into microfluidic channels. The *in situ* patterning of the two proteins onto the interior of a permanently bonded PDMS microfluidic device has been shown to improve immunoaffinity-based tumor cell capture.[66] Micropatterned photopolymerized poly(acrylic acid) (PAA) with carboxyl termini on the PDMS microchannels was used for E-selectin attachment using 1-ethyl-3-(3-dimethylaminopropyl)carbodiimide (EDC)/*N*-hydroxysulfosuccinimide (NHS) coupling. Then, the self-assembled monolayers of (3-mercaptopropyl)trimethoxysilane with sulfhydryl groups backfilled between the PAA patterns on the PDMS microchannels were used for surface immobilization of the anti-EpCAM–dendrimer conjugates using an *N*-γ-maleimidobutyryl-oxysuccinimide ester (GMBS) cross-linker (Fig. 3c). By patterning the two adhesive proteins in an alternating manner, the specificity and sensitivity for tumor cell capture were significantly increased under flow. This *in situ* pattern of alternating biomimetic proteins reduced the leukocyte capture by up to 82%, while maintaining a high tumor cell capture efficiency up to 1.9 times higher than that of a surface with anti-EpCAM only. Moreover, this patterning technique requires no mask alignment and can be used to spatially control the immobilization of multiple proteins inside a sealed microchannel.

2.2.4. Incorporation of releasing capability. CTCs captured from patients' blood provide opportunities to perform post-capture analysis to identify signaling pathways and investigate the molecular profiling of individual CTCs. A number of approaches to efficiently release the captured CTCs have been explored to facilitate subsequent cell culture and single-cell analyses.[67,68] A promising approach is to use stimuli-responsive polymers for CTC capture and release. The stimuli-responsive polymers have been used to release the captured CTCs upon exposure to various stimuli, such as light, temperature, pH and physical stress. Proteolytic enzymes and/or

stimuli-responsive polymers have been commonly used to engineer the CTC capture surface to release the cells as a result of surface degradation or in response to external stimuli.

Alginate hydrogels have been incorporated onto the surface to increase the CTC capture efficiency by altering the surface topography and efficiently release the isolated CTCs from the surface upon simple stimulation. Alginate in a solution containing $CaCl_2$ was injected into the 1st generation CTC-chip for *in situ* hydrogel formation on the chip surface, which was further functionalized with a mixture of PEG, EDC, sulfo-NHS and anti-CD34. This ionically crosslinked hydrogel was used to capture and release CD34-expressing endothelial progenitor cells in heparin-treated blood specimens without the need for enzymatic digestion,[67] with the principle of calcium chelation driving the substrate degradation. When the alginate hydrogel on the chip surface was covalently crosslinked using an Irgacure 2959 photoinitiator and functionalized with anti-EpCAM, EpCAM-expressing CTCs were captured and released *via* treatment with alginate lyase (Fig. 4a).[69] This calcium-sensitive approach is limited by the fact that chelating agents, such as ethylenediaminetetraacetic acid (EDTA), cannot be used as blood anticoagulants. The use of enzymes (alginate lyase and DNase) has also resulted in poor efficiency (<10%) of release and limited viability of the cells.[57]

Self-assembled DNA nanostructures were incorporated onto an avidin-coated, herringbone microfluidic device *via* rolling circle amplification at 37 °C using a biotinylated primer–circular template complex, nucleotide triphosphate containing deoxyribose (dNTP) and DNA polymerase (Fig. 4b).[70] Multiple long aptamers in the matrix of the DNA nanostructures on the chip had a highly specific binding affinity with lymphoblastic CCRF-CEM cells over monovalent aptamers and anti-EpCAM.[70] The degradation of the DNA matrix upon exposure to DNases/endonucleases induced the release of captured cells from the chip.[70]

As discussed earlier in section 2.2.1, the thermally responsive NanoVelcro system demonstrated the effective capture and release of tumor cells from blood upon external temperature changes. In this study, thermally responsive poly(*N*-isopropylacrylamide) (PNIPAAm) polymers were grafted onto a silicon nanowire array (SiNWA)-based CTC detection platform.[57] The amino groups on the PNIPAAm-grafted NanoVelcro were then conjugated with biotin-NHS and streptavidin for further functionalization with biotinylated anti-EpCAM. As shown in Fig. 4c, this thermally responsive platform demonstrated the effective capture of tumor cells in the presence of human blood cells at 37 °C and release of the captured cells with retained viability and functionality at 4 °C. The PNIPAAm-grafted NanoVelcro exhibited reversible cellular attachment and detachment in response to temperature changes due to the transition of the chain conformation between the hydrophobic collapsed state and the hydrophilic extended state. At 37 °C, biotins were present on the surfaces, leading to the binding of biotinylated anti-EpCAM through streptavidin as a bridge and thus facilitating the capture of

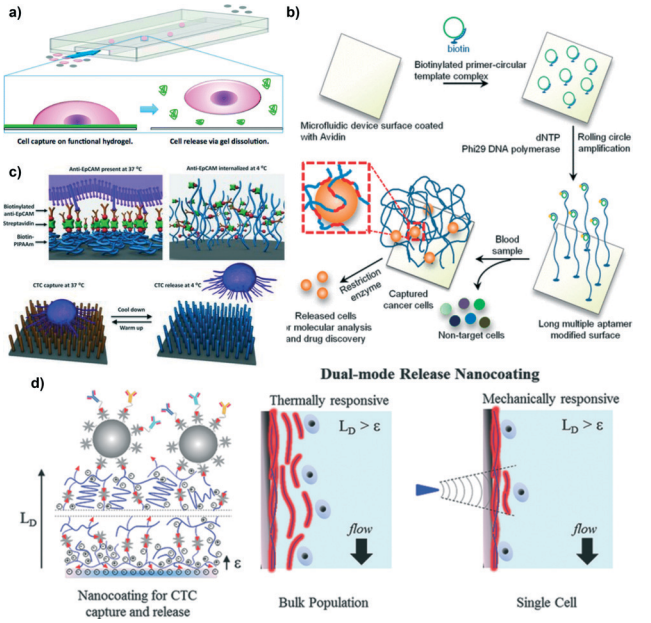

Fig. 4 Releasing capability-integrated microfluidic devices for CTC capture and release. (a) An alginate gel-coated microfluidic device was able to capture CTCs after anti-EpCAM functionalization, as well as release the captured CTCs *via* gel dissolution after brief exposure to the bacterial enzyme, alginate lyase (reproduced with permission from the American Chemical Society). (b) A microfluidic device incorporated with long multivalent DNA aptamers isolated CTCs from whole blood, which were released after DNase treatment to cleave the DNA aptamers on the surface (reproduced with permission from the National Academy of Sciences). (c) A schematic illustration of a microfluidic device integrated with a nanostructured silicon surface and thermally responsive polymers, such as PNIPAAm. The captured CTCs on the nanomaterial-based device at 37 °C were released after lowering the temperature to 4 °C (reproduced with permission from Wiley-VCH Verlag GmbH & Co. KGaA, Weinheim). (d) The multiple layer-by-layer deposition of biotinylated gelatin and streptavidin on the surface of a microfluidic device induced the isolation and release of CTCs from the nanocoating in two different mechanisms: bulk cell release *via* temperature changes (left) and single-cell/selective release after applying localized shear stress *via* inducing vibration from the microtip (right) (reproduced with permission from Wiley-VCH Verlag GmbH & Co. KGaA, Weinheim).

cancer cells with high efficiency. As the temperature decreased to 4 °C, the PNIPAAm chains became hydrophilic and extended to encapsulate anti-EpCAM, which stimulated the release of captured cells.

A thermally responsive gelatin-based nanostructured coating formed by the layer-by-layer (LbL) deposition of biotinylated gelatin and streptavidin was also developed for the temperature-responsive release (for bulk-population recovery) of captured CTCs (Fig. 4d).[68] Raising the device temperature to 37 °C degraded the nanocoating from the whole surface within minutes for the bulk-population release of CTCs. In addition, the local regions in the gelatin nanocoating were sensitive to mechanical stress from a frequency-controlled microtip, which was used for the mechanosensitive single-cell release of CTCs (Fig. 4d).[68] This dual release strategy of the gelatin-coated chip has successfully driven the

characterization of the PIK3CA and EGFR oncogene mutations in the released CTCs.

Although promising, it should be noted that these stimuli-responsive nanomaterials may face challenges in order to be clinically implemented due to the requirement of running the samples at certain temperatures (for thermally responsive nanomaterials) and under specified conditions (DNase/endonuclease-free conditions for DNA/aptamer-based materials). Additionally, the exposure of individual cells to a certain stimulus (*e.g.* enzyme, light, chemical, temperature or mechanical stress) during the release process may affect the cell viability. In addition, the nanomaterial-integrated microfluidic device may have some potential issues regarding stability and quality control due to the intrinsic heterogeneous and often unstable characteristics of nanomaterials.

2.3. *In situ* or sequential analysis of isolated CTCs

The genetic information of enumerated CTCs at the single-cell level will significantly contribute to a better understanding of the CTC population through complete characterization and functional analysis. The single-cell genetics of low-frequency CTCs may provide the means to link genetic data to new insights into the complex mechanisms of drug resistance, ultimately leading to the development of personalized cancer treatments. Research incorporating microfluidics and single-cell genetic analysis, including cell capture and enrichment, cell compartmentalization and detection, can be used to create simple and more informative tools for CTC studies.[71] Microfluidic technologies are attractive for single-cell manipulation due to their precise handling in isolating rare CTCs and low risk of contamination from the environment and components within the sample.[12] Microfluidic single-cell techniques can also allow for high-throughput and detailed genetic analyses that increase accuracy with reduced cost, compared to bulk techniques.[12] Additionally, microfluidic technologies provide an additional alternative to *in situ* culture of live and intact CTCs for downstream analysis due to the unique properties of PDMS such as optical transparency, flexibility, and high permeability to gases, water, oxygen and chemicals.[52,72] Incorporating these microfluidic platforms into research and clinical laboratory workflows can fulfill an unmet need in biology, delivering highly accurate and informative data necessary to develop new therapies and monitor patient outcomes.

2.3.1. *In situ* analysis while capturing. Enrichment must be conducted in line with a separation system to reduce the contamination possibilities and the liquid volume for rapid detection and analysis. To clean up unnecessary hematological cells, a variety of detection strategies, such as layers with 8 μm pores for size-based filtration[73] and magnetic or physical traps,[74] were incorporated into microfluidic systems for CTC detection and *in situ* analysis. Optically transparent PDMS microfluidic devices allow the identification of captured and washed CTCs through immunofluorescence staining against cytokeratin, CD45 and DAPI on-chip, and subsequent *in situ* analysis to be carried out for the single-cell genetic profiling of the CTCs.

Fluorescence *in situ* hybridization (FISH) has been frequently used for *in situ* analysis and successfully evaluated the amplification status of cancer-related genes in microfluidic devices. The 2nd generation CTC chip with a herringbone pattern[75] was used to successfully isolate pancreatic CTCs from mouse and human blood, and investigate the molecular characterization of signaling pathways associated with proliferation and anoikis (a form of programmed cell death that is induced by anchorage-dependent cells detaching from the surrounding extracellular matrix) (Fig. 5a).[76] Expression of WNT in pancreatic cancer cells is known to suppress anoikis, enhance anchorage-independent sphere formation, and increase the metastatic propensity *in vivo*.[76] The results of single-molecule RNA sequencing showed the amplification of WNT signaling genes of captured CTCs in 5 out of 11 cases of pancreatic cancer patients, demonstrating that the WNT signaling pathways may contribute to pancreatic cancer metastasis. The treatment of WNT inhibitors, TAK1 inhibitors and shTak1 on tumor cells clearly showed increased anchorage-independent tumor sphere formation. Thus, the effectiveness of WNT inhibition in suppressing this effect could potentially identify a novel drug target for metastasis suppression to prevent the distal spread of cancer.[75]

2.3.2. Sequential analysis. By concentrating rare cells in localized regions using microfluidic systems, mechanical traps are some of the most commonly used methods for anchoring particles and cells to a physical structure and enabling multistep perfusion of reagents to perform cell assays on-chip. After capture, it is important to release particles and cells on-demand for further downstream analysis.[74,77] Having discussed the application of stimuli-responsive polymers for the release of captured cells from microfluidic devices in section 2.2.4, this section will focus on other approaches to collecting CTCs for downstream, sequential analyses.

Swennenhuis, J. F. *et al.* developed a microfluidic device with microwells to capture and recover CTCs.[74] The captured and identified CTCs on the multiwell microfluidic device were collected by punching the bottom of the device. The self-seeding chip contained 6400 microwells (with a diameter of 70 μm and a depth of 360 μm) to trap a single cell per well (Fig. 5b). A 5 μm pore-size filter was placed in the center of the microwell to allow media or non-target cells to pass through, removing unnecessary background signals. After a fast and efficient distribution of single cells in individual microwells by applying a negative pressure of 10 mbar under the slide using an air pump, a manometer and a pressure regulator, the cells of interest in the microwells were recovered in a 96 PCR well plate by punching the 1 μm thick bottom. The recovered cells were used for DNA amplification and Sanger sequencing.[74] The signatures of the ROBO2 and PTEN genes in the recovered PC-3 cells were identified, which were used to determine the capture specificity.[74] Apart from punching the wall of the microfluidic device, other

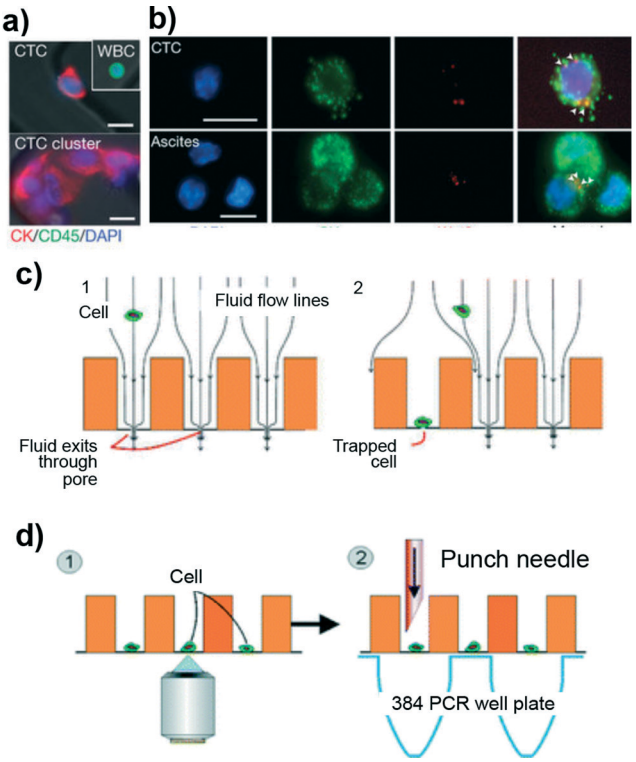

Fig. 5 Microfluidic device applications for *in situ* or sequential analysis of the captured CTCs. (a and b) Immunofluorescence staining (a) and RNA *in situ* hybridization (RNA-ISH) (b) of mouse pancreatic CTCs on the microfluidic device. (a) Green-labelled leukocytes and red-labelled CTC clusters were identified *in situ* (DAPI, blue; cytokeratin (CK), red; CD45, green). (b) RNA-ISH of CTCs showed the co-expression of CK8+18 (green) and WNT2 (red) transcripts (reproduced with permission from Nature Publishing Group). (c and d) Direct collection of single CTCs per microwell for sequential analysis. (c) While leukocytes or other blood components were passing through a small hole at the bottom, the CTCs were trapped in the microwell with a diameter of 70 μm and a depth of 360 μm. After identifying the trapped cells as CTCs, single cells per microwell were acquired in a 384 well plate by punching the silicon bottom using a punch needle (reproduced with permission from the Royal Society of Chemistry).

approaches, including the use of a suction needle for single-cell retrieval, could be also combined with microfluidic devices to recover the captured CTCs for sequential analysis.[78]

Conclusions

Accurate CTC detection has great potential to provide valuable clinical insight into the progress of metastatic cancers and monitor the responses of patients during cancer therapy. As summarized in this review, recent advances in microfluidics such as miniaturization of bench-top analytical instruments, integration with nanotechnology and *in situ* analysis of captured CTCs, have provided various designs and promising implementation of highly reliable CTC-capture platforms with excellent yield and selectivity. However, microfluidic devices, especially those that are PDMS-based, have potential difficulties to be translated for clinical impact. For clinical translation, the next generation of CTC microfluidic devices is expected to meet the following standards: (i) enhanced detection sensitivity and specificity than the current CTC devices; (ii) shorter total analysis time for CTC detection, capture and identification; (iii) enhanced capability for *in situ* or sequential analysis after capture; (iv) simplification of operating procedures for high throughput; (v) minimal batch-to-batch variations. Beyond simple enumeration, *in situ* analysis of captured CTCs in microfluidic devices will lead to novel insight into cancer progression and metastasis, and genetic/phenotypic changes in cancer cells. We expect that such CTC microfluidic devices will be implemented for routine use in point-of-care testing and ultimately play a key role in achieving personalized therapeutics for cancer patients.

Acknowledgements

This work was supported by the National Cancer Institute (NCI), National Institutes of Health (NIH) (grant no. R01-CA182528), the National Science Foundation (NSF) (grant no. DMR-1409161) and the Technological Innovation R&D Program (grant no. S2083505) funded by the Small and Medium Business Administration of Korea.

References

1 S. Riethdorf, H. Fritsche, V. Muller, T. Rau, C. Schindlbeck, B. Rack, W. Janni, C. Coith, K. Beck, F. Janicke, S. Jackson, T. Gornet, M. Cristofanilli and K. Pantel, *Clin. Cancer Res.*, 2007, **13**, 920–928.
2 M. Cristofanilli, G. T. Budd, M. J. Ellis, A. Stopeck, J. Matera, M. C. Miller, J. M. Reuben, G. V. Doyle, W. J. Allard, L. W. Terstappen and D. F. Hayes, *N. Engl. J. Med.*, 2004, **351**, 781–791.
3 A. van de Stolpe, K. Pantel, S. Sleijfer, L. W. Terstappen and J. M. den Toonder, *Cancer Res.*, 2011, **71**, 5955–5960.
4 S. Paget, *Cancer Metastasis Rev.*, 1989, **8**, 98–101.
5 J. H. Myung, K. A. Gajjar, Y. E. Han and S. P. Hong, *Polym. Chem.*, 2012, **3**, 2336–2341.
6 J. H. Myung, K. A. Tam, S. Park, A. Cha and S. Hong, *Wiley Interdiscip. Rev.: Nanomed. Nanobiotechnol.*, 2015, DOI: 10.1002/wnan.1360.
7 N. Saucedo-Zeni, S. Mewes, R. Niestroj, L. Gasiorowski, D. Murawa, P. Nowaczyk, T. Tomasi, E. Weber, G. Dworacki, N. G. Morgenthaler, H. Jansen, C. Propping, K. Sterzynska, W. Dyszkiewicz, M. Zabel, M. Kiechle, U. Reuning, M. Schmitt and K. Lucke, *Int. J. Oncol.*, 2012, **41**, 1241–1250.
8 W. J. Allard, J. Matera, M. C. Miller, M. Repollet, M. C. Connelly, C. Rao, A. G. Tibbe, J. W. Uhr and L. W. Terstappen, *Clin. Cancer Res.*, 2004, **10**, 6897–6904.
9 A. J. Armstrong, M. S. Marengo, S. Oltean, G. Kemeny, R. L. Bitting, J. D. Turnbull, C. I. Herold, P. K. Marcom, D. J. George and M. A. Garcia-Blanco, *Mol. Cancer Res.*, 2011, **9**, 997–1007.

10 S. K. Arya, B. Lim and A. R. Rahman, *Lab Chip*, 2013, **13**, 1995–2027.
11 I. Cima, C. Wen Yee, F. S. Iliescu, W. M. Phyo, K. H. Lim, C. Iliescu and M. H. Tan, *Biomicrofluidics*, 2013, **7**, 11810.
12 Y. Dong, A. M. Skelley, K. D. Merdek, K. M. Sprott, C. Jiang, W. E. Pierceall, J. Lin, M. Stocum, W. P. Carney and D. A. Smirnov, *J. Mol. Diagn.*, 2013, **15**, 149–157.
13 P. R. Gascoyne and S. Shim, *Cancers*, 2014, **6**, 545–579.
14 V. Gupta, I. Jafferji, M. Garza, V. O. Melnikova, D. K. Hasegawa, R. Pethig and D. W. Davis, *Biomicrofluidics*, 2012, **6**, 24133.
15 C. Jin, S. M. McFaul, S. P. Duffy, X. Deng, P. Tavassoli, P. C. Black and H. Ma, *Lab Chip*, 2014, **14**, 32–44.
16 L. Hajba and A. Guttman, *Trends. Analyt. Chem.*, 2014, **59**, 9–16.
17 P. N. Nge, C. I. Rogers and A. T. Woolley, *Chem. Rev.*, 2013, **113**, 2550–2583.
18 J. El-Ali, P. K. Sorger and K. F. Jensen, *Nature*, 2006, **442**, 403–411.
19 C. D. Chin, V. Linder and S. K. Sia, *Lab Chip*, 2012, **12**, 2118–2134.
20 B. Hong and Y. L. Zu, *Theranostics*, 2013, **3**, 377–394.
21 P. Chen, Y. Y. Huang, K. Hoshino and X. Zhang, *Lab Chip*, 2014, **14**, 446–458.
22 S. Zheng, H. Lin, J. Q. Liu, M. Balic, R. Datar, R. J. Cote and Y. C. Tai, *J. Chromatogr. A*, 2007, **1162**, 154–161.
23 G. Attard, M. Crespo, A. C. Lim, L. Pope, A. Zivi and J. S. de Bono, *Clin. Cancer Res.*, 2011, **17**, 3048–3049; author reply 3050.
24 L. S. Lim, M. Hu, M. C. Huang, W. C. Cheong, A. T. Gan, X. L. Looi, S. M. Leong, E. S. Koay and M. H. Li, *Lab Chip*, 2012, **12**, 4388–4396.
25 A. Yusa, M. Toneri, T. Masuda, S. Ito, S. Yamamoto, M. Okochi, N. Kondo, H. Iwata, Y. Yatabe, Y. Ichinosawa, S. Kinuta, E. Kondo, H. Honda, F. Arai and H. Nakanishi, *PLoS One*, 2014, **9**, e88821.
26 D. L. Adams, P. X. Zhu, O. V. Makarova, S. S. Martin, M. Charpentier, S. Chumsri, S. H. Li, P. Amstutz and C. M. Tang, *RSC Adv.*, 2014, **4**, 4334–4342.
27 J. H. Myung, M. Roengvoraphoj, K. A. Tam, T. Ma, V. A. Memoli, E. Dmitrovsky, S. J. Freemantle and S. Hong, *Anal. Chem.*, 2015, **87**, 10096–10102.
28 D. Marrinucci, K. Bethel, R. H. Bruce, D. N. Curry, B. Hsieh, M. Humphrey, R. T. Krivacic, J. Kroener, L. Kroener, A. Ladanyi, N. H. Lazarus, J. Nieva and P. Kuhn, *Hum. Pathol.*, 2007, **38**, 514–519.
29 B. Molnar, A. Ladanyi, L. Tanko, L. Sreter and Z. Tulassay, *Clin. Cancer Res.*, 2001, **7**, 4080–4085.
30 N. Aceto, A. Bardia, D. T. Miyamoto, M. C. Donaldson, B. S. Wittner, J. A. Spencer, M. Yu, A. Pely, A. Engstrom, H. Zhu, B. W. Brannigan, R. Kapur, S. L. Stott, T. Shioda, S. Ramaswamy, D. T. Ting, C. P. Lin, M. Toner, D. A. Haber and S. Maheswaran, *Cell*, 2014, **158**, 1110–1122.
31 A. F. Sarioglu, N. Aceto, N. Kojic, M. C. Donaldson, M. Zeinali, B. Hamza, A. Engstrom, H. Zhu, T. K. Sundaresan, D. T. Miyamoto, X. Luo, A. Bardia, B. S. Wittner, S. Ramaswamy, T. Shioda, D. T. Ting, S. L. Stott, R. Kapur, S. Maheswaran, D. A. Haber and M. Toner, *Nat. Methods*, 2015, **12**, 685–691.
32 A. J. Mach, O. B. Adeyiga and D. Di Carlo, *Lab Chip*, 2013, **13**, 1011–1026.
33 A. J. Mach, J. H. Kim, A. Arshi, S. C. Hur and D. Di Carlo, *Lab Chip*, 2011, **11**, 2827–2834.
34 J. Che, A. J. Mach, D. E. Go, I. Talati, Y. Ying, J. Rao, R. P. Kulkarni and D. Di Carlo, *PLoS One*, 2013, **8**, e78194.
35 A. M. Dupuy, S. Lehmann and J. P. Cristol, *Clin. Chem. Lab. Med.*, 2005, **43**, 1291–1302.
36 F. Olasagasti and J. C. Ruiz de Gordoa, *Transl. Res.*, 2012, **160**, 332–345.
37 S. Nagrath, L. V. Sequist, S. Maheswaran, D. W. Bell, D. Irimia, L. Ulkus, M. R. Smith, E. L. Kwak, S. Digumarthy, A. Muzikansky, P. Ryan, U. J. Balis, R. G. Tompkins, D. A. Haber and M. Toner, *Nature*, 2007, **450**, 1235–1239.
38 S. L. Stott, C. H. Hsu, D. I. Tsukrov, M. Yu, D. T. Miyamoto, B. A. Waltman, S. M. Rothenberg, A. M. Shah, M. E. Smas, G. K. Korir, F. P. Floyd, Jr., A. J. Gilman, J. B. Lord, D. Winokur, S. Springer, D. Irimia, S. Nagrath, L. V. Sequist, R. J. Lee, K. J. Isselbacher, S. Maheswaran, D. A. Haber and M. Toner, *Proc. Natl. Acad. Sci. U. S. A.*, 2010, **107**, 18392–18397.
39 J. H. Kang, S. Krause, H. Tobin, A. Mammoto, M. Kanapathipillai and D. E. Ingber, *Lab Chip*, 2012, **12**, 2175–2181.
40 E. Ozkumur, A. M. Shah, J. C. Ciciliano, B. L. Emmink, D. T. Miyamoto, E. Brachtel, M. Yu, P. I. Chen, B. Morgan, J. Trautwein, A. Kimura, S. Sengupta, S. L. Stott, N. M. Karabacak, T. A. Barber, J. R. Walsh, K. Smith, P. S. Spuhler, J. P. Sullivan, R. J. Lee, D. T. Ting, X. Luo, A. T. Shaw, A. Bardia, L. V. Sequist, D. N. Louis, S. Maheswaran, R. Kapur, D. A. Haber and M. Toner, *Sci. Transl. Med.*, 2013, **5**, 179ra147.
41 J. M. Oatley, M. J. Oatley, M. R. Avarbock, J. W. Tobias and R. L. Brinster, *Development*, 2009, **136**, 1191–1199.
42 K. Hoshino, Y. Y. Huang, N. Lane, M. Huebschman, J. W. Uhr, E. P. Frenkel and X. Zhang, *Lab Chip*, 2011, **11**, 3449–3457.
43 N. M. Karabacak, P. S. Spuhler, F. Fachin, E. J. Lim, V. Pai, E. Ozkumur, J. M. Martel, N. Kojic, K. Smith, P. I. Chen, J. Yang, H. Hwang, B. Morgan, J. Trautwein, T. A. Barber, S. L. Stott, S. Maheswaran, R. Kapur, D. A. Haber and M. Toner, *Nat. Protoc.*, 2014, **9**, 694–710.
44 J. H. Shin, M. G. Lee, S. Choi and J.-K. Park, *RSC Adv.*, 2014, **4**, 39140–39144.
45 R. M. Mohamadi, J. D. Besant, A. Mepham, B. Green, L. Mahmoudian, T. Gibbs, I. Ivanov, A. Malvea, J. Stojcic, A. L. Allan, L. E. Lowes, E. H. Sargent, R. K. Nam and S. O. Kelley, *Angew. Chem., Int. Ed.*, 2015, **54**, 139–143.
46 P. G. Schiro, M. Zhao, J. S. Kuo, K. M. Koehler, D. E. Sabath and D. T. Chiu, *Angew. Chem., Int. Ed.*, 2012, **51**, 4618–4622.
47 M. Zhao, B. Wei, W. C. Nelson, P. G. Schiro and D. T. Chiu, *Lab Chip*, 2015, **15**, 3391–3396.
48 H. Becker, *Lab Chip*, 2010, **10**, 271–273.

49 J. Balsam, H. A. Bruck and A. Rasooly, *Analyst (Cambridge, U. K.)*, 2014, **139**, 4322–4329.
50 K. A. Hyun and H. I. Jung, *Lab Chip*, 2014, **14**, 45–56.
51 J. C. McDonald, D. C. Duffy, J. R. Anderson, D. T. Chiu, H. Wu, O. J. Schueller and G. M. Whitesides, *Electrophoresis*, 2000, **21**, 27–40.
52 P. C. H. Li, *Microfluidic lab-on-a-chip for chemical and biological analysis and discovery*, Taylor & Francis/CRC Press, Boca Raton, 2006.
53 Q. Yu, H. Liu and H. Chen, *J. Mater. Chem. B*, 2014, **2**, 7849–7860.
54 L. Wang, W. Asghar, U. Demirci and Y. Wan, *Nano Today*, 2013, **8**, 347–387.
55 S. Wang, H. Wang, J. Jiao, K. J. Chen, G. E. Owens, K. Kamei, J. Sun, D. J. Sherman, C. P. Behrenbruch, H. Wu and H. R. Tseng, *Angew. Chem., Int. Ed.*, 2009, **48**, 8970–8973.
56 S. Wang, K. Liu, J. Liu, Z. T. Yu, X. Xu, L. Zhao, T. Lee, E. K. Lee, J. Reiss, Y. K. Lee, L. W. Chung, J. Huang, M. Rettig, D. Seligson, K. N. Duraiswamy, C. K. Shen and H. R. Tseng, *Angew. Chem., Int. Ed.*, 2011, **50**, 3084–3088.
57 S. Hou, H. C. Zhao, L. B. Zhao, Q. L. Shen, K. S. Wei, D. Y. Suh, A. Nakao, M. A. Garcia, M. Song, T. Lee, B. Xiong, S. C. Luo, H. R. Tseng and H. H. Yu, *Adv. Mater.*, 2013, **25**, 1547–1551.
58 A. E. Saliba, L. Saias, E. Psychari, N. Minc, D. Simon, F. C. Bidard, C. Mathiot, J. Y. Pierga, V. Fraisier, J. Salamero, V. Saada, F. Farace, P. Vielh, L. Malaquin and J. L. Viovy, *Proc. Natl. Acad. Sci. U. S. A.*, 2010, **107**, 14524–14529.
59 J. Autebert, B. Coudert, J. Champ, L. Saias, E. T. Guneri, R. Lebofsky, F.-C. Bidard, J.-Y. Pierga, F. Farace, S. Descroix, L. Malaquin and J.-L. Viovy, *Lab Chip*, 2015, **15**, 2090–2101.
60 M. Mammen, S. K. Choi and G. M. Whitesides, *Angew. Chem., Int. Ed.*, 1998, **37**, 2755–2794.
61 S. Hong, P. R. Leroueil, I. J. Majoros, B. G. Orr, J. R. Baker, Jr. and M. M. Banaszak Holl, *Chem. Biol.*, 2007, **14**, 107–115.
62 J. H. Myung, K. A. Gajjar, J. Saric, D. T. Eddington and S. Hong, *Angew. Chem., Int. Ed.*, 2011, **50**, 11769–11772.
63 J. H. Myung, K. A. Gajjar, J. H. Chen, R. E. Molokie and S. Hong, *Anal. Chem.*, 2014, **86**, 6088–6094.
64 J. H. Myung, C. A. Launiere, D. T. Eddington and S. Hong, *Langmuir*, 2010, **26**, 8589–8596.
65 J. H. Myung, K. A. Gajjar, R. M. Pearson, C. A. Launiere, D. T. Eddington and S. Hong, *Anal. Chem.*, 2011, **83**, 1078–1083.
66 C. Launiere, M. Gaskill, G. Czaplewski, J. H. Myung, S. Hong and D. T. Eddington, *Anal. Chem.*, 2012, **84**, 4022–4028.
67 A. Hatch, G. Hansmann and S. K. Murthy, *Langmuir*, 2011, **27**, 4257–4264.
68 E. Reategui, N. Aceto, E. J. Lim, J. P. Sullivan, A. E. Jensen, M. Zeinali, J. M. Martel, A. J. Aranyosi, W. Li, S. Castleberry, A. Bardia, L. V. Sequist, D. A. Haber, S. Maheswaran, P. T. Hammond, M. Toner and S. L. Stott, *Adv. Mater.*, 2015, **27**, 1593–1599.
69 A. M. Shah, M. Yu, Z. Nakamura, J. Ciciliano, M. Ulman, K. Kotz, S. L. Stott, S. Maheswaran, D. A. Haber and M. Toner, *Anal. Chem.*, 2012, **84**, 3682–3688.
70 W. A. Zhao, C. H. Cui, S. Bose, D. G. Guo, C. Shen, W. P. Wong, K. Halvorsen, O. C. Farokhzad, G. S. L. Teo, J. A. Phillips, D. M. Dorfman, R. Karnik and J. M. Karp, *Proc. Natl. Acad. Sci. U. S. A.*, 2012, **109**, 19626–19631.
71 A. M. Thompson, A. L. Paguirigan, J. E. Kreutz, J. P. Radich and D. T. Chiu, *Lab Chip*, 2014, **14**, 3135–3142.
72 S. Halldorsson, E. Lucumi, R. Gomez-Sjoberg and R. M. T. Fleming, *Biosens. Bioelectron.*, 2015, **63**, 218–231.
73 C.-L. Chang, W. Huang, S. I. Jalal, B.-D. Chan, A. Mahmood, S. Shahda, B. H. O'Neil, D. E. Matei and C. A. Savran, *Lab Chip*, 2015, **15**, 1677–1688.
74 J. F. Swennenhuis, A. G. J. Tibbe, M. Stevens, M. R. Katika, J. van Dalum, H. Duy Tong, C. J. M. van Rijn and L. W. M. M. Terstappen, *Lab Chip*, 2015, **15**, 3039–3046.
75 M. Yu, D. T. Ting, S. L. Stott, B. S. Wittner, F. Ozsolak, S. Paul, J. C. Ciciliano, M. E. Smas, D. Winokur, A. J. Gilman, M. J. Ulman, K. Xega, G. Contino, B. Alagesan, B. W. Brannigan, P. M. Milos, D. P. Ryan, L. V. Sequist, N. Bardeesy, S. Ramaswamy, M. Toner, S. Maheswaran and D. A. Haber, *Nature*, 2012, **487**, 510–513.
76 S. M. Frisch and R. A. Screaton, *Curr. Opin. Cell Biol.*, 2001, **13**, 555–562.
77 L. Li, W. M. Liu, J. C. Wang, Q. Tu, R. Liu and J. Y. Wang, *Electrophoresis*, 2010, **31**, 3159–3166.
78 D. E. Campton, A. B. Ramirez, J. J. Nordberg, N. Drovetto, A. C. Clein, P. Varshavskaya, B. H. Friemel, S. Quarre, A. Breman, M. Dorschner, S. Blau, C. A. Blau, D. E. Sabath, J. L. Stilwell and E. P. Kaldjian, *BMC Cancer*, 2015, **15**, 360.